

Simultaneous observation of a traveling vortex structure in the morning sector and a field line resonance in the postnoon sector

D. R. McDiarmid,¹ T. K. Yeoman,² I. F. Grant,³ and W. Allan⁴

Abstract. Radar observations suggesting ULF field line resonances impulsively excited via a cavity or waveguide mode were obtained simultaneously in the dawn (Bistatic Auroral Radar System (BARS)) and postnoon (Sweden and Britain Radar-Auroral Experiment (SABRE)) sectors. The primary data used to study this event are from both the European Incoherent Scatter magnetometer cross and Subauroral Magnetometer Network magnetometer arrays in the postnoon sector and from the Canadian Auroral Network for the Origin of Plasmas in the Earth's Neighborhood Program Unified Study (CANOPUS), Magnetometer, RIometer and tellurics Array (MARIA), the GOES 7 magnetometer, and the neural network classification of Defense Meteorological Satellite Program (DMSP) particle data in the dawn sector. In the postnoon sector (Scandinavia) a decaying field line resonance was observed following a more complicated initial interval. The resonance period was 326 s (3.07 mHz). However, in the dawn sector the response was dominated by the initial interval in which the characteristics of a traveling vortex system were observed. The subsequent disturbance in this sector was of lesser amplitude and without discerned pattern. The field-aligned current(s) of the traveling vortex structure was (were) at about 65° Eccentric Dipole Field Line (EDFL) latitude (approximately 68° International Geomagnetic Reference Field (IGRF)). The DMSP neural network data, however, indicate this position to have been well within the magnetosphere. GOES 7 was on a field line which was connected to the ionosphere near the MARIA meridian line at about 62.5° EDFL latitude (approximately 65.5° IGRF), just equatorward of the traveling vortex structure. It observed a magnetic disturbance which was initially driven and followed directly by a damped sinusoid signature of the azimuthal component. The frequency during this decay was 4.45 mHz (225-s period). Values of Σ_p , the height-integrated Pedersen conductivity for both the postnoon and GOES 7 damped segments were deduced. These were low, particularly if the disturbances were in the second harmonic along the field line as suggested by GOES 7 data, and perhaps imply an additional loss mechanism. Although substantially understood, this pulsation event had distinctly different characteristics in the two time sectors and displayed many puzzling features. In particular, it was significantly more complicated than our initial anticipation of global excitation of field line resonances via a cavity or waveguide mode.

Introduction

The transient magnetohydrodynamic response of the magnetospheric cavity to impulsive excitation has been the subject of a number of observational studies [e.g., *Nopper et al.*, 1982; *Baumjohann et al.*, 1984; *Allan et al.*, 1985; *Crowley et al.*, 1987, 1989; *Potemra et al.*, 1989]. The response to such excitation has also recently been the subject

of a considerable volume of theoretical and modeling studies, principally concerned with the coupling of field line resonances (FLR) with compressional mode cavity resonances [*Allan et al.*, 1986a, b, 1987; *Kivelson and Southwood*, 1986; *Inhester*, 1987; *Krauss-Varban and Patel*, 1988; *Zhu and Kivelson*, 1988; *Lee and Lysak*, 1991; *Lysak and Lee*, 1992]. (We note that for some of these works the word "cavity" should be replaced by "waveguide", as pointed out by *Samson et al.* [1992] and *Walker et al.* [1992], since a traveling wave in the azimuthal direction was assumed. We have altered the wording below as appropriate.)

The present observational study arose from a simulation of the signature expected from a magnetospheric waveguide (cavity) mode in auroral radar data by *McDiarmid and Allan* [1990], such as the Scandinavian Twin Auroral Radar Experiment (STARE) [*Greenwald et al.*, 1978] or the Sweden and Britain Radar-Auroral Experiment (SABRE) [*Nielsen et al.*, 1983]. A transient wave signature reminiscent of those simulated by *McDiarmid and Allan* [1990] was found in the SABRE Wick radar data and was subsequently

¹Herzberg Institute of Astrophysics, National Research Council, Ottawa, Ontario, Canada.

²Ionospheric Physics Group, Department of Physics and Astronomy, Leicester University, Leicester, England.

³Department of Physics, University of Western Ontario, London, Canada.

⁴National Institute of Water and Atmospheric Research, Lower Hutt, New Zealand.

discovered to exist simultaneously in the Bistatic Auroral Radar System (BARS) [McNamara *et al.*, 1983] Red Lake radar data. This event is examined in the next section. The range of observational instrumentation used in this analysis includes ground-based radar and magnetometer data from the European and Canadian sectors and magnetometer data from two geostationary spacecraft. This large range of observations has revealed a complex wave structure, both spatially and temporally. It will be seen that this structure is significantly more complicated than that expected for a pulsation excited via a cavity or waveguide mode. A number of features of the observed wave can be understood within the context of current theoretical and modeling work on hydro-magnetic wave coupling in the magnetosphere, but a number of puzzling features of the disturbance remain.

Instrumentation and Analysis

The wave event occurred between 1400 and 1500 UT on March 14, 1990, and was observed by a number of instruments widely separated in local time and latitude. (All times hereafter in this paper are UT unless otherwise specified.) Radar observations are available in both the dawn sector at approximately 0800 LT (via BARS) and in the afternoon sector at approximately 1530 LT (via SABRE). Unfortunately, in both cases only line-of-sight velocities and backscatter intensities from one radar were available from the Red Lake and Wick stations of the BARS and SABRE systems, respectively. Data from both these radars have been augmented by extensive ground magnetometer support. Twelve stations of the Magnetometer, RIometer and tellurics Array (MARIA) portion of the Canadian Auroral Network for the Origin of Plasmas in the Earth's Neighborhood Unified Study (CANOPUS) ground array contribution to the International Solar Terrestrial Physics (ISTP) program were in the morning sector [e.g., Grant *et al.*, 1992] (covering local times approximately 0500–0830 LT). In the afternoon sector there were 14 stations, split evenly between the United Kingdom Subauroral Magnetometer Network (SAMNET) [Yeoman *et al.*, 1990] and the European Incoherent Scatter (EISCAT) magnetometer cross [Lühr *et al.*, 1984] array (approximately 1500–1630 LT). This ground-based instrumentation covers L shells from $L = 2.6$ to $L > 10$ and spans 11 hours in local time. These extensive ground data are augmented by geostationary orbit magnetic field data from the GOES 6 and 7 spacecraft [Rufenach *et al.*, 1992] at local times of approximately 0530 and approximately 0730 LT, respectively. The geographic and geomagnetic coordinates of the ground-based instrumentation employed in this study are given in Table 1. Note that both International Geomagnetic Reference Field (IGRF) and Eccentric Dipole Field Line (EDFL) [Wallis *et al.*, 1982; Grant *et al.*, 1992] magnetic coordinates are used.

The European sector SABRE radar at Wick is a VHF coherent radar operating at 153 MHz with a field of view covering some 200,000 km². The radar measures the backscatter intensity and Doppler velocity from ionospheric E region electron density irregularities in fifty 20-km range gates in each of eight antenna beams with a temporal resolution of 20 s for the data in this study. The Canadian BARS radar is a similar system but operates at 48 MHz with a sampling interval for the data in this study of 30 s. The SAMNET, EISCAT magnetometer cross, and MARIA

magnetometers are all fluxgate instruments (the MARIA instruments are ring-core fluxgates). SAMNET and MARIA have a sampling interval of 5 s, and the EISCAT magnetometer cross has 20-s sampling. The geostationary orbit magnetic field data have a sampling interval of 3.06 s. In this study the geostationary orbit magnetic field data are examined in a slowly time-varying field-aligned coordinate system. In this system a time-varying background field is defined by low-pass filtering the three components of the field with a filter having a sharp cutoff at 2-mHz. A right-handed and orthogonal time-varying coordinate system (H_p , H_r , H_a) is then defined using the low-pass-filtered data with one axis aligned along the time-varying background field (H_p). H_a is then the azimuthal component (positive eastward), which is in the direction of the cross product of the background field and the satellite geocentric position vector. The radial component H_r completes the set and is positive outward. This coordinate system is similar to that used by Yumoto *et al.* [1990]. The filter cutoff frequency was chosen to be below the major peaks in the spectra of the data in the original (H_p , H_r , H_n) coordinate system. The footprint of the GOES 7 spacecraft, mapped down to the E region ionosphere with the Tsyganenko [1989] field model, lies in latitude between the MARIA stations ISLL and GILL. GOES 6 lies some 2 hours to the west of GOES 7. The reverse mapping of all the sites to the magnetic equatorial plane yields Figure 1.

The Event

Background

The Kp during the event was 5-, and in the previous 12 hours it varied between 30 and 5+. The period was thus moderately disturbed and near to both the equinox and solar maximum. The prevailing Dst was -32 nT. This interval in fact lay well into the recovery phase of a magnetic storm with a maximum Dst excursion of -159 nT just prior to 0000 on March 13, 1990.

Data

The radar data for this event are illustrated in Figure 2, together with a simulation performed by McDiarmid and Allan [1990] for comparison. The presentation is in the range-time-intensity (RTI) format. The SABRE data (Figure 2c) suggested that the phase change along the radar beam increased during the lifetime of the wave packet, a characteristic feature of pulsations driven by magnetospheric waveguide (cavity) modes (and also of individually ringing field lines), as noted by McDiarmid and Allan [1990]. There is also a clear difference between adjacent (positive and negative Doppler velocity) backscatter intensity peaks, characteristic of a wave observed with a DC velocity offset. A similar, although shorter-lived and thus more ambiguous, signature is observed in the BARS data (Figure 2b). A subsequently corrected instrumental problem in the BARS system at the lowest detectable backscatter intensities [Grant *et al.*, 1992] makes it difficult to determine the exact threshold in Figure 2b. The pulsation is observed first in the SABRE data at approximately 1409, approximately 3 min before the first BARS detection of the wave. However, this time lag may be simply a consequence of differing radar sensitivity.

Table 1. Coordinates of the Ground-Based Instrumentation Employed in This Study

Station	Code Name	Geographic Lat, °N	Geographic Long, °E	EDFL Lat, °N	EDFL Long, °E	Geomagnetic Lat, °N	Geomagnetic Long, °E	<i>L</i> Shell
<i>Subauroral Magnetometer Network (SAMNET)</i>								
Faroe	FAR	62.05	352.98	123.3	12.3	60.76	78.13	4.26
Glenmore	GML	57.16	356.32			54.92	78.03	3.08
York	YOR	53.95	358.95			50.97	78.63	2.56
Nordli	NOR	64.37	13.36			61.29	95.33	4.40
Kvistaberg	KVI	59.50	17.63			55.84	96.03	3.22
Oulu	OUL	65.10	25.85			61.32	105.63	4.41
Nurmijärvi	NUR	60.51	24.66			56.60	102.26	3.35
<i>European Incoherent Scatter (EISCAT) Cross</i>								
Sørøya	SOR	70.54	22.22			67.02	106.94	6.67
Alta	ALT	69.86	22.96			66.30	106.87	6.29
Kautokeino	KAU	69.02	23.05			65.45	106.21	5.89
Muonio	MUO	68.01	23.53			64.40	105.77	5.44
Pello	PEL	66.90	24.08			63.24	105.39	5.01
Kilpisjärvi	KIL	69.05	20.70			65.62	104.45	5.96
Kevo	KEV	69.76	27.01			65.97	109.86	6.13
<i>Sweden and Britain Radar-Auroral Experiment (SABRE)</i>								
		63.6-	0.0-			60.5-	84.5-	4.5
		68.6	12.0			66.9	97.5	6.6
<i>Canadian Auroral Network for the Open Program Unified Study (CANOPUS): Magnetometer, Rlometer and tellurics Array (MARIA)</i>								
Rankin Inlet	RANK	62.82	267.89	70.37	338.92	73.18	332.53	12.13
Eskimo Point	ESKI	61.11	265.95	68.62	336.47	71.42	329.72	10.01
Churchill	FCHU	58.76	265.92	66.27	336.68	69.17	330.33	8.04
Back	BACK	57.72	265.83	65.23	336.67	68.17	330.43	7.35
Gillam	GILL	56.38	265.36	63.88	336.21	66.84	329.97	6.57
Island Lake	ISLL	53.86	265.34	61.39	336.42	64.39	330.41	5.44
Pinawa	PINA	50.20	263.96	57.73	335.08	60.65	328.91	4.23
Contwoyto Lake	CONT	65.75	248.75	72.39	311.30	73.27	300.15	12.26
Fort Smith	FSMI	60.02	248.05	66.56	313.21	67.70	303.30	7.06
Fort McMurray	FPCM	56.66	247.79	63.23	315.30	64.37	304.64	5.43
Meanoak	MEAN	54.62	246.67	61.00	313.31	62.13	304.11	4.65
Rabbit Lake	RABB	58.22	256.32	65.33	324.38	67.44	315.64	6.90
Fort Simpson	FSIM	61.76	238.77	67.40	300.58	67.45	290.80	6.91
Dawson City	DAWS	64.05	220.89	67.32	277.48	65.78	270.98	6.04
<i>Bistatic Auroral Radar Study (BARS)</i>								
		55.3-	263.0-	63.0-	333.0-	66.1-	323.4-	6.2
		60.2	268.9	67.8	340.5	71.1	336.7	9.6
Bjornoja		74.5	19.2			71.13	109.29	9.71

Lat, latitude; long, longitude; EDFL, Eccentric Dipole Field Lines. Geomagnetic coordinates and *L* shells are calculated using the International Geomagnetic Reference Field for 1990.3 at 120 km. For EDFL coordinates, see Wallis *et al.* [1982] and Grant *et al.* [1992].

Ground magnetometer data from observatories in the local time sectors of the two radars are displayed in Figures 3 and 4. Figure 3 displays the *H* and *D* components of the European sector magnetograms from the combined SAMNET and EISCAT magnetometer cross arrays. Figure 4 displays *X* and *Y* components from the MARIA stations. (For the MARIA meridian line the EDFL *X* and *Y* axes are almost identical with the *H* and *D* axes.) The European (afternoon) sector magnetograms show the pulsation to have a very clear ground magnetometer signature with the pulsation onset occurring at approximately 1405. The *H* component is dominant with a maximum peak-to-peak amplitude of approximately 250 nT occurring at KAU (*L* = 5.9). The *D* component also has significant amplitude, typically 70–80% of the *H* component. The wave packet structure in Figure 3 clearly changes with time from a complicated initial section (before approximately 1418) to a damped sinusoid appearance thereafter. From onset to approximately 1418 the wave is of a different frequency and more broadband character than that after 1418. In this latter interval the pulsation shows little evidence of frequency variation across a wide range of *L* shells (*L* = 2.6–6.7) in the continental European

sector. It will be seen below, however, that the data recorded in the United Kingdom sector (FAR, GML, YOR) differed somewhat from that recorded at similar geomagnetic latitudes on the continent. In the Canadian (morning) sector a quite different signature is observed. Here the pulsation onset in the magnetometer data is not clear and occurs perhaps as early as 1408 or as late as 1410+. The signature, again, has a clear amplitude maximum, in this case a peak-to-peak maximum of approximately 300 nT at BACK (*L* = 7.5). The MARIA data exhibit a trend to lower frequency along the latitudinal chain from ISLL to FCHU.

The azimuthal phase propagation of the radar and magnetometer wave signatures has been examined using phase measurements obtained from a curve-fitting technique and also results from a cross-correlation technique. In both cases an antisunward azimuthal propagation was deduced, which is to say, eastward phase propagation in the European sector and westward phase propagation in the Canadian sector.

The magnetic field data from the two geostationary orbit spacecraft are displayed in Figure 5. The pulsation onset measured on the spacecraft was either delayed or simultaneous with respect to the ground-observed onset, in so far as

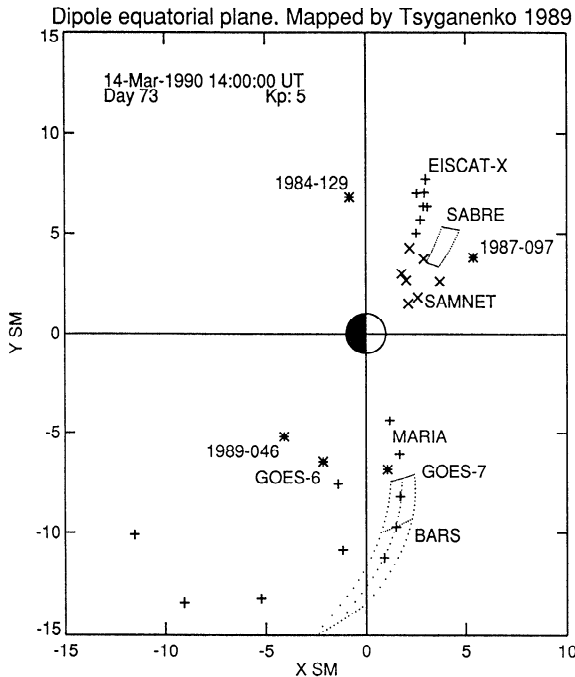


Figure 1. Location at the magnetic equatorial plane of the field lines passing through the observing sites used in this paper.

the latter can be determined. The wave first became distinctly apparent at approximately 1410+ at GOES 7. The beginning of the disturbance at GOES 6 is more difficult to ascertain relative to the background, but it was close to 1410+. The wave is initially seen most strongly at GOES 7, as 1-2 wave cycles in the field-aligned H_f satellite coordinate, from 1410-1418. During this interval the radial H_r and azimuthal H_a components exhibit a growing amplitude. Subsequently, the clearest signature is in the azimuthal component H_a which resembles a damped sinusoid. During the initial interval, H_r was mostly in antiphase with H_f and H_a initially lagged H_f by about 90° . The wave disturbance is much less clear in the GOES 6 spacecraft, partially because of its lower amplitude. However, H_f and H_r show a pulse in antiphase between about 1410- and 1412. Thereafter, the oscillation in H_a is most apparent, although of considerably lower amplitude relative to that seen at GOES 7.

Analysis Techniques

A number of analytical tools were employed. These included analytic signal analysis and nonlinear curve fitting of one of a number of predefined functions to the data, as well as the production of maximum entropy method (MEM) spectra and wave polarization plots. Various approaches were examined to remove baseline effects from the MEM spectra. It was decided in the end to remove the mean plus a linear trend. The MEM order used was 25% of the data length, unless otherwise noted.

Analytic signal analysis has been clearly described by Walker *et al.* [1992]. In some cases our signal spectra did not have isolated peaks, and it was questionable how well filtering could separate the various spectral components. This tool was often used as a backup to other techniques.

The nonlinear curve fitting involved the use of up to three damped sinusoids. The fit parameters were the amplitudes, damping constants, frequencies, and phases. The mean and linear trend could also be included. The number of sinusoids was chosen in advance, and there was an option to preset the frequencies.

European Sector

We have already noted above that the magnetograms from the Scandinavian sector appear to be monochromatic after about 1418 when the disturbance was similar to a damped sinusoid. Prior to 1418 the signals were highly structured, as if several perturbations had occurred. This behavior is reflected in the MEM spectra for these data (Figures 6a and 6b). Figure 6a shows spectra for the interval 1404 to 1420 for the European data and 1410 to 1418 for the Canadian data, whereas Figure 6b shows spectra for 1420 to 1434 for the European data and 1418 to 1430 for the Canadian data. Note that the latter spectra for the European sector are single peaked near 3 mHz, whereas the former are almost always double peaked. (FAR, GML, and YOR are United Kingdom sector stations. Data from these stations differ from those obtained in Scandinavia, as is indicated in Figure 6 and is discussed below.) Figure 7 shows spectra of the SABRE Wick station radar data for the latter 1420 to 1434 interval; these peaks are also at about 3 mHz. Analytic signal analysis of high-pass-filtered (2-mHz corner frequency) magnetometer data also indicated a complex wave packet structure prior to about 1418 and a monochromatic signal with declining amplitude following this interval.

Nonlinear curve fitting of a single damped sinusoid to the data over the post 1419:40 interval yielded frequencies clustered about 3.07 mHz (326-s period). This strengthened the impression arrived at above that the disturbance was monochromatic during that interval in the Scandinavian sector. A second curve fitting of a damped sinusoid to the data over the interval 1419:40 to 1436:40 with the frequency

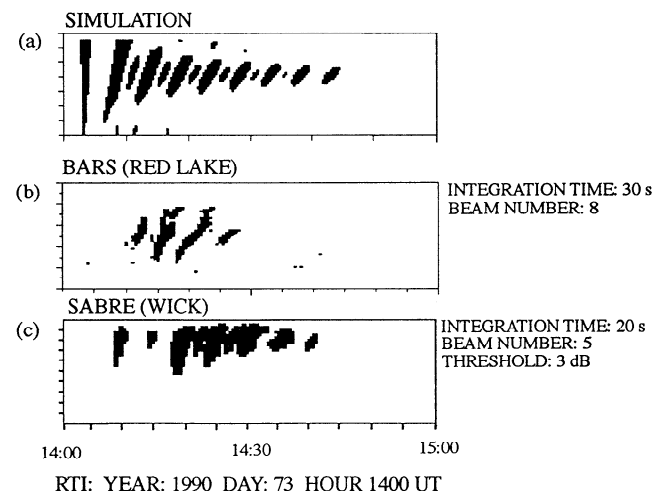


Figure 2. Range-time-intensity (RTI) plots (a) simulated for a waveguide-excited field line resonance [McDiarmid and Allan, 1990] and for the March 14, 1990, pulsation event using (b) Bistatic Auroral Radar System (BARS) and (c) Sweden and Britain Radar Auroral Experiment (SABRE) data.

EISCAT-X and SAMNET 14-Mar-1990

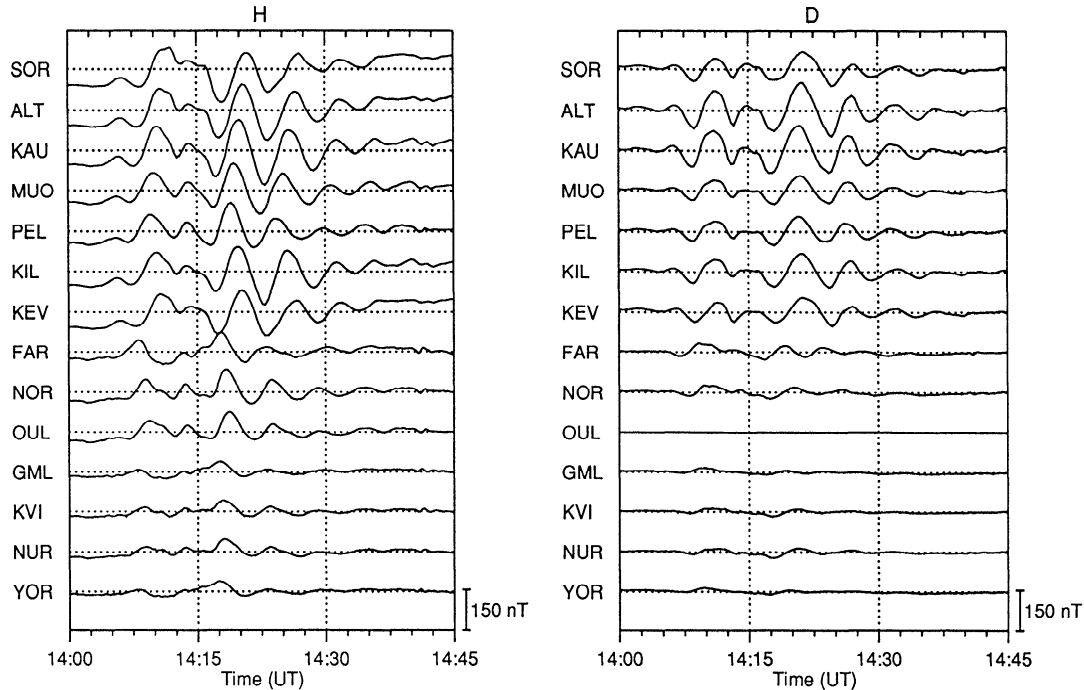


Figure 3. *H* and *D* components of the European sector magnetograms from the combined European Incoherent Scatter (EISCAT) and Subauroral Magnetometer Network (SAMNET) magnetometer cross arrays for the event on March 14, 1990.

fixed at 3.07 mHz was then performed. The results are shown in Figure 8. Points marked *w* and *e* in Figure 8 (open symbols) are for stations west and east of the meridian line, respectively, i.e., *w* are KIL, NOR, and KVI; *e* is KEV. The curves in Figure 8 suggest a field line resonance near 66° geomagnetic latitude. The *H* component latitudinal amplitude profile is broadened by the spatial integration of ionospheric current implicit in ground-based magnetic records [Hughes and Southwood, 1976].

Analysis of SABRE time sequences as a function of longitude at several latitudes revealed an eastward phase propagation of the event with an azimuthal wave number *m* in the range 5 to 8. Although the data did not permit an

accurate determination of *m*, there appeared to be a tendency for *m* to increase with latitude. This appearance may be related to the range dependent character of the SABRE RTI plot in Figure 2, which gives the impression of a period variation with latitude, even though the spectra do not show this dependence. However, these results pertain to the SABRE field of view which is over the North Sea [see Nielsen *et al.*, 1983, Figure 2]. The magnetometer data from Scandinavia, on the other hand, are more consistent with *m* values of less than or equal to approximately 3. This discrepancy may be due in part to the large error inherent in these *m* determinations but possibly also to an increase of the phase velocity with longitude eastward.

MARIA (EDFL DATA) 14-Mar-1990

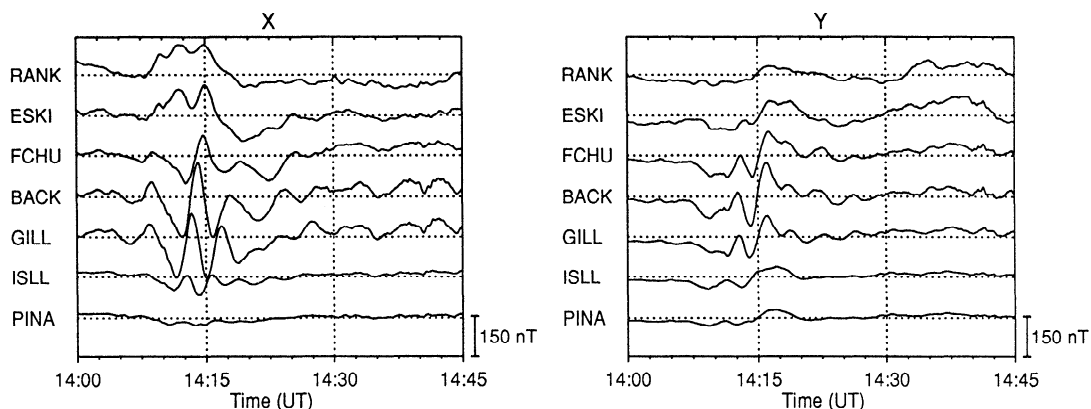


Figure 4. MAgnetometer, RIometer and tellurics Array (MARIA) *X* and *Y* component magnetograms for the event in Eccentric Dipole Field Line (EDFL) orientation. In this sector the *X* and *Y* components are very close to the *H* and *D* components.

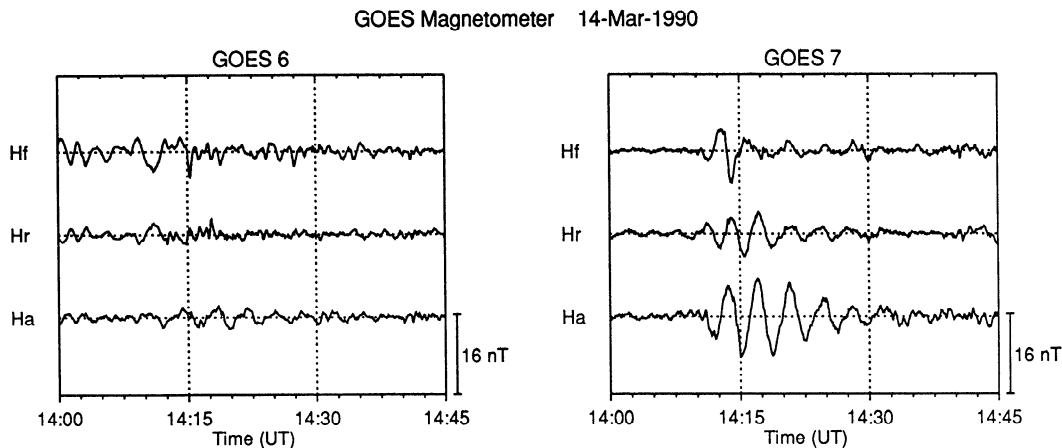


Figure 5. Magnetic field variation observed on (left) GOES 6 and (right) GOES 7.

The damping decrements shown in Figure 8 seem rather large; large enough that one wonders if they correspond to reasonable values of height-integrated Pedersen conductivity Σ_p , assuming Joule heating to be the only significant loss mechanism. There are two ways to estimate Σ_p under the assumption that energy is lost only to Joule heating, since both the width of the latitude profile and the damping rate are related to Σ_p , although the profile width is also dependent on the radial variation of the cold plasma mass distribution in the magnetosphere.

Using the curves of *Newton et al.* [1978] as well as their scaling relations for a change in cold plasma mass density, we have estimated Σ_p under the assumptions that the damped oscillation observed after 1418 was either fundamental or second harmonic along the field line, and that the observed damping rate is the Joule loss value. That is to say, we assume on the one hand that there is no continuous flow of energy into the resonance to compensate for the ionospheric damping and, on the other hand, that there was no other significant damping mechanism. (We will consider the alternatives below.) The results of *Cummings et al.* [1969] were used to convert guided poloidal mode frequencies to toroidal mode frequencies. Although the Cummings et al. calculations were for 67° geomagnetic and our pulsation peaked at 66° , the error introduced is thought to be acceptable for the level of accuracy expected. The average value of γ/ω for the H component was close to 0.11, and this value was used. The values of Σ_p obtained were 5 S for the fundamental and 3 S for the second harmonic. These compare with about 8 S as predicted by the empirical model of *Wallis and Budzinski* [1981]. The results above thus seem to be reasonably consistent with a field line resonance in the fundamental mode along the field line, although as we will see, the GOES 7 data suggest otherwise. If the oscillation was actually in the second harmonic, then the Σ_p predicted above is low, which implies that the observed damping decrement is large. This matter is discussed further below, where it is concluded that the second harmonic is more likely.

On the basis of a comparison of the H component latitudinal amplitude profile in Figure 8 with those presented by *Hughes and Southwood* [1976], it is estimated that the approximately 4.5° half-amplitude width corresponds to a

resonance width of about 2° above the ionosphere. Using the expressions of *Walker* [1979] along with his data [*Walker*, 1980, Figure 8], we estimate Σ_p to be 3 S for an oscillation in the fundamental along the magnetic field. Given the greater uncertainty of a Σ_p determination based on latitudinal width, particularly when the latter is only an estimate, and the fact that the radial variation of cold plasma density is unknown, we conclude that the observed profile width is not inconsistent with the observed damping rates.

Note that the polarization near the amplitude profile peak in Figure 8 is not linear or even close to it, as *Samson et al.* [1971] have suggested it should be. Samson et al. concluded that pulsation polarization reverses from counterclockwise through linear to clockwise (CW), moving poleward in the morning sector and the reverse of this in the afternoon sector. However, not all observations coincide with this expectation. For instance, *Poulter* [1982] examined three field line resonances seen in STARE data and found that two were close to linear at all latitudes and the remaining one had a reversal of polarization well away from peak amplitude. *Nielsen* [1984] observed a resonance associated with a sunward propagating wave on the magnetopause, and the polarization was CW everywhere except poleward of the resonance where it approached linear. In our case the polarization was CW and became linear near the equatorward limit of the profile. These situations seem consistent with the observations of *Rostoker and Sullivan* [1987], who found that Pc 5's in the postnoon sector often do not display the characteristics described by *Samson et al.* [1971].

It was implied above that the pulsation behaved differently in the United Kingdom sector from what was seen in Scandinavia. Curve fitting and, particularly, analytic signal analysis show that the United Kingdom sector H components all experienced a similar change of frequency with time. From 1418 the frequency decreased until about 1425 when the trend reversed, and the frequency then increased until about 1432. The mean frequency was about 3.1 mHz. Also, the single damped sinusoid variable frequency fits to the United Kingdom data yielded periods for the H components which were consistently larger than 326 s and periods for the D components which were consistently smaller. Given the reasonable overlap in geomagnetic latitude of the FAR and GML United Kingdom sector stations with the NOR and

KVI Scandinavian stations, these results point toward a change with longitude rather than latitude. Explanations of magnetic disturbance latitude profiles of field line resonances have traditionally been in terms of azimuthal variations which involve only phase. Magnetometers are, of course, sensitive to off-meridian ionospheric currents, and thus more complicated azimuthal variations introduce some uncertainty into profile interpretation. We don't know what influence the different behavior evident in the United Kingdom sector may have had on the results shown in Figure 8 or if the change in this sector extended to higher latitudes.

The peak in the D component profile in Figure 8 might be due in part to the orientation of the resonance shell in the ionosphere being rotated CW from perpendicular to the magnetometer meridian to a line oriented from the north of west to south of east. In other words, the EISCAT/SAMNET magnetometer meridian line may not have crossed the resonance shell at right angles. Using the data in Figure 8, we found that such a rotation through 10° to 15° produces an increased poloidal (D) component amplitude equatorward of the resonance and a diminished amplitude near the resonance. In addition, the contribution of the east-west phase change to our slightly out-of-meridian profile is to increase the phase change of the toroidal (H) component through the resonance. Thus if our meridian profile was out of meridian as suggested, one would expect a latitudinal phase change of the H component greater than or equal to the upper limit of 180° normally expected. This is consistent with the large phase change implied in Figure 8.

Canadian Sector

Comparison of Figures 3 and 4 shows that the disturbance seen over central North America along the MARIA meridian line differs from that seen over Scandinavia. Along the MARIA line the disturbance was dominant in the 1410 to 1418 interval. The Scandinavian disturbance in this initial interval did not dominate the whole anything like the disturbance seen by MARIA did. Furthermore, the disturbance in the post-1418 interval over the MARIA line does not show the characteristics of a field line resonance.

Comparison of magnetic disturbance spectra (Figures 6a and 6b) also shows a difference in the response observed at the two meridians. In the 1410 to 1418 interval the dominant peaks of the MARIA line X component spectra decrease monotonically in frequency from 6 mHz at ISLL to 2+ mHz at RANK. Comparison of the X component spectra with the magnetograms reveals, however, that the dominant low-frequency spectral peaks for RANK and ESKI correspond to the 6+-min excursion of this component between 1410- and 1416+ at these two stations. The lower-amplitude peaks at about 5.7 mHz correspond to the lower-amplitude, shorter-period oscillations which ride upon these excursions. The EISCAT magnetometer cross H component spectra for the initial interval, on the other hand, are double peaked throughout at about 1.5 and 3.5 mHz. In the second or 1418 to 1430 interval the MARIA line X and Y component spectra are either single-peaked or double-peaked, with many of the peaks around 2.5 and 4.5 mHz, compared with the monochromatic behavior in the Scandinavian sector. In neither interval, however, do the spectral peaks of the two horizontal components for each MARIA site correspond well to each other. This is in distinct contrast to the EISCAT magnetometer cross spectra in the right-hand side of Figure 6b.

The distinctive feature of MARIA latitudinal line magnetograms are the strong oscillations between about 1412 and 1417 which are clearly related across an extended interval of latitude. Following this interval the oscillations appear to be less monochromatic and are clearly of lesser amplitude. This behavior is reminiscent of that shown by the data of *Friis-Christensen et al.* [1988a]. We thus plotted our data in their traveling vortex format [see *Friis-Christensen et al.*, 1988a, Figure 4]. The data were high-pass filtered with a 0.56-mHz cutoff to be consistent with their analysis, and the result is shown in Figure 9 along with another plot presenting data high-pass filtered with a 2-mHz cutoff frequency. Figure 9 here is similar to that of *Friis-Christensen et al.* [1988a, Figure 4]. Cross correlation between MARIA X component data from stations separated in longitude and comparison of BARS grid point data from different longitudes indicate that the traveling vortex structure propagated westward at a velocity between 5 and 10 km/s. There is a suggestion that this velocity may have changed with longitude.

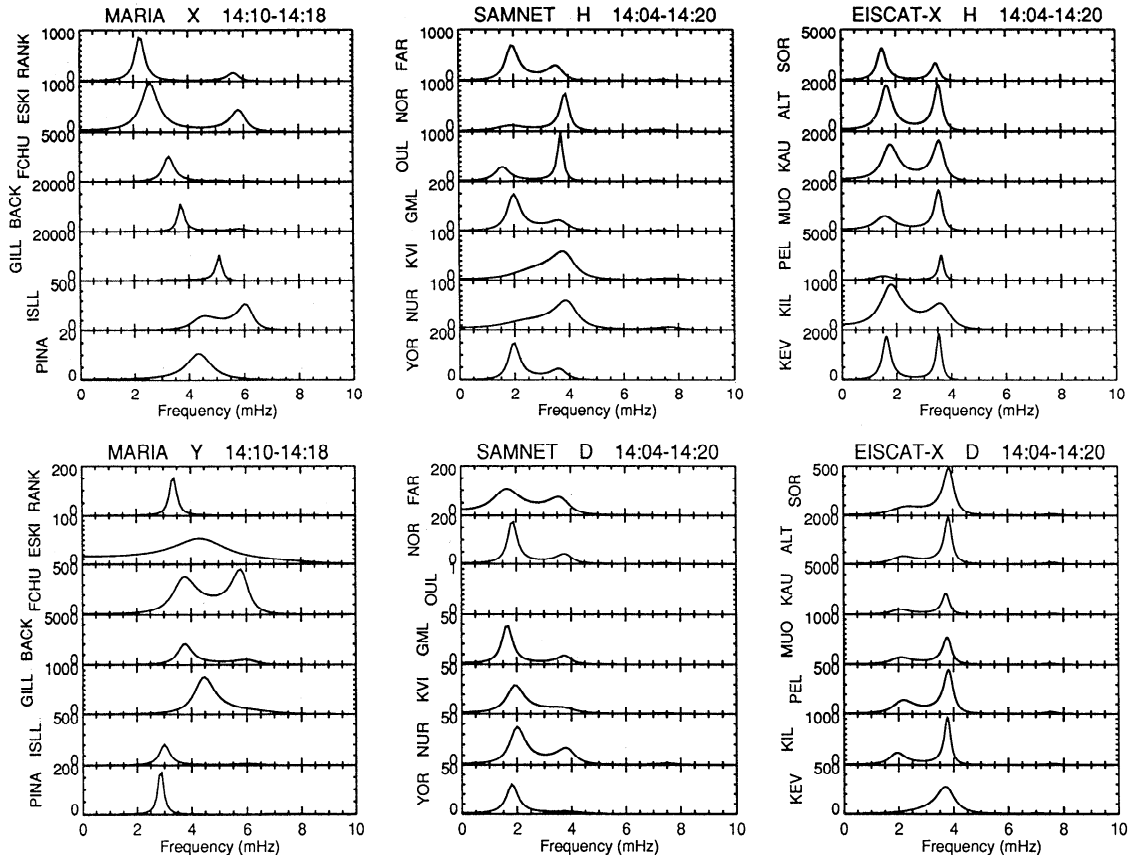
Figure 9 shows two clear and coherent patterns, both between the horizontal X and Y components and between stations. However plotted, the disturbance is greatest above the GILL, BACK, and FCHU stations. The 0.56-mHz cutoff plot indicates a vortex structure having a single, downward field-aligned current centered at about 64.5° EDFL embedded in another disturbance. The 2-mHz cutoff plot, on the other hand, yields a pattern indicating a twin vortex system having a pair of field-aligned currents centered at about 65.5° EDFL and separated by about 840 km. (The velocities given above correspond to a separation lying between 550 and 1100 km.) The westward (eastward) of these currents was upward (downward), consistent with the passage of a solar wind pressure pulse over the magnetopause [*Friis-Christensen et al.*, 1988a; *Glassmeier and Heppner*, 1992]. In the absence of information about the amplitude and nature of the background disturbance which seems to have been present it is very difficult to deduce the actual structure. Unfortunately, IMP 8 data which might have helped clarify this question do not exist for the interval following 1400 on this day. Thus it may be concluded that a vortex system of some sort passed over this sector, but the detail of its structure is unresolved.

The ground magnetometer data thus have the appearance of containing a driven MHD response in the form of the traveling vortex structure followed by a complex decaying transient. One might have expected this transient to consist primarily of damped oscillation of individual field lines in the toroidal mode at their own resonant frequency. This would be the toroidal mode transient associated with the exit or turnoff of the vortex generator. *Poulter and Allan* [1985] have simulated what should be expected as the ground-based magnetic record of such a transient. They showed that the spatial integration implicit in such data causes the peak of any latitudinal variation of transient response amplitude in the ionosphere to be broadened in the ground record. They also showed that the magnetic record will indicate a significantly reduced variation of frequency with latitude and a larger damping rate than actually pertains to the field oscillations. On the other hand, their simulated magnetograms were well represented by single damped sinusoids.

Our data for the post-1418 interval had none of these characteristics. As noted above, the X and Y component spectra are not consistent with the *Poulter and Allan* [1985] picture. The magnetograms (Figure 4) do not look like

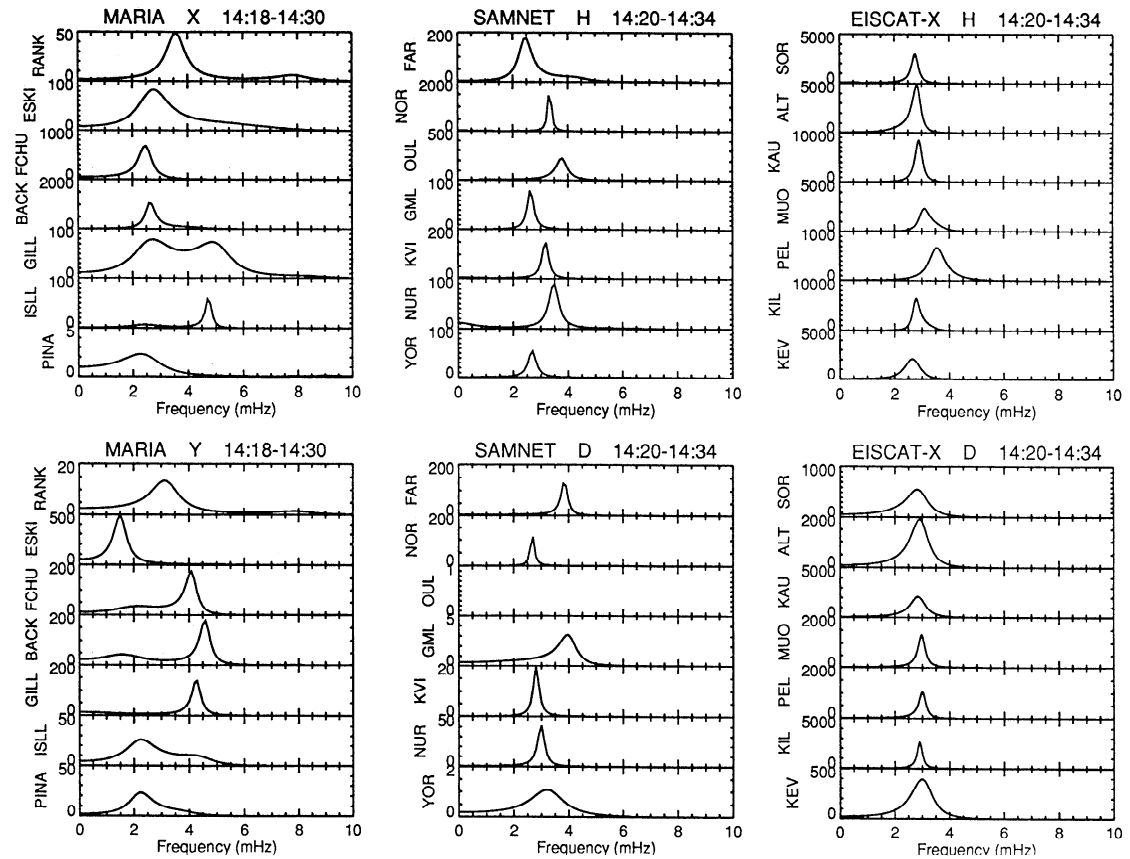
14-Mar-1990 MEM spectra

a



14-Mar-1990 MEM spectra

b



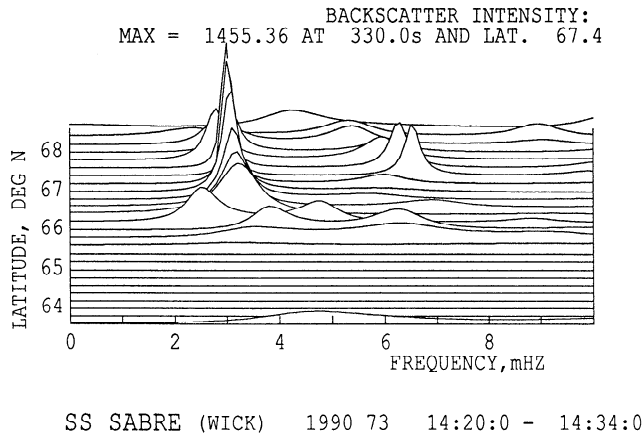


Figure 7. MEM spectra of the SABRE Wick radar data as a function of latitude.

single damped sinusoids, and curve fitting confirmed this observation. Often, the sum of two damped sinusoids was required to achieve a good fit. Single sinusoids seldom fitted well to the data, and multiple-sinusoid fits often yielded a growing component. With two or more sinusoids there was no overall clear and consistent pattern of frequency variation with latitude. There was, however, a clear tendency for one of the frequencies to be near 4.4 mHz for all reasonably good fits to any of the BACK, GILL, and ISLL components. This result is consistent with most of the MEM spectra obtained for this interval for these stations. The spectra for the 1355 to 1405 interval (not shown), however, are not inconsistent with the possibility that a spectral component close to this frequency existed prior to the disturbance.

DMSP F9 passed 5° to the east of FCHU at about 1431 and directly overhead of RANK shortly thereafter. The neural network classification of the DMSP particle data [Newell *et al.*, 1991] places the Central Plasma Sheet/Boundary Plasma Sheet (CPS/BPS) boundary near FCHU and the BPS/mantle boundary much poleward of RANK. Thus what we have denoted as a traveling vortex structure seems to have been deeply embedded in the magnetosphere, contrary to what might have been expected. (DMSP data for the Friis-Christensen *et al.* [1988a] observations are inconclusive in this respect. The fact that the sequence CPS, BPS, LLBL, mantle, BPS, LLBL, mantle, (where LLBL denotes the low latitude boundary layer) is given for the nearest pass in time indicates that human interpretation of the DMSP data is probably required for reliable boundary interpretation in their case. All of these regions occurred over Greenland on a poleward pass which went from west of Iceland to north of Thule.)

Figure 6. Maximum entropy method (MEM) spectra for selected intervals of the horizontal magnetic disturbance observed by the EISCAT magnetometer cross, SAMNET, and MARIA magnetometer arrays. Time intervals are (a) 1404-1420 UT for European data and 1410-1418 UT for Canadian data and (b) 1420-1434 UT for European data and 1418-1430 UT for Canadian data.

GOES 6 and 7 Data

The MEM spectra for the 1410-1418 and 1418-1430 intervals of the GOES 6 and 7 magnetograms (Figure 5) are shown in Figure 10. The appearance of the GOES 7 H_r and H_a components in particular are clearly consistent with these spectra. The magnetic footprint of GOES 7 was between the latitudes of ISLL and GILL but somewhat to the west, as indicated by Figure 1. It is thus interesting to note that the GOES 7 spectral peaks are close to 4.4 mHz, particularly in the second interval. It is therefore clear that the GOES 7 field line was oscillating at a frequency detected in data from magnetically nearby ground stations.

Figure 5 shows that the toroidal mode disturbance H_a seen at GOES 7 first grew in amplitude from about 1411 to perhaps 1417 in association with the main disturbance in the compressional component H_r . Thereafter, H_a decayed in amplitude. The H_r/H_a polarization also varied from an initial circle of growing radius through an ellipse to linear polarization after about 1417. It is as though the toroidal oscillation was driven by the compressional disturbance prior to 1417, after which it decayed by energy loss to the ionosphere and possibly elsewhere.

Curve fitting of a linear trend plus a damped sinusoid to these data yielded results consistent with this description.

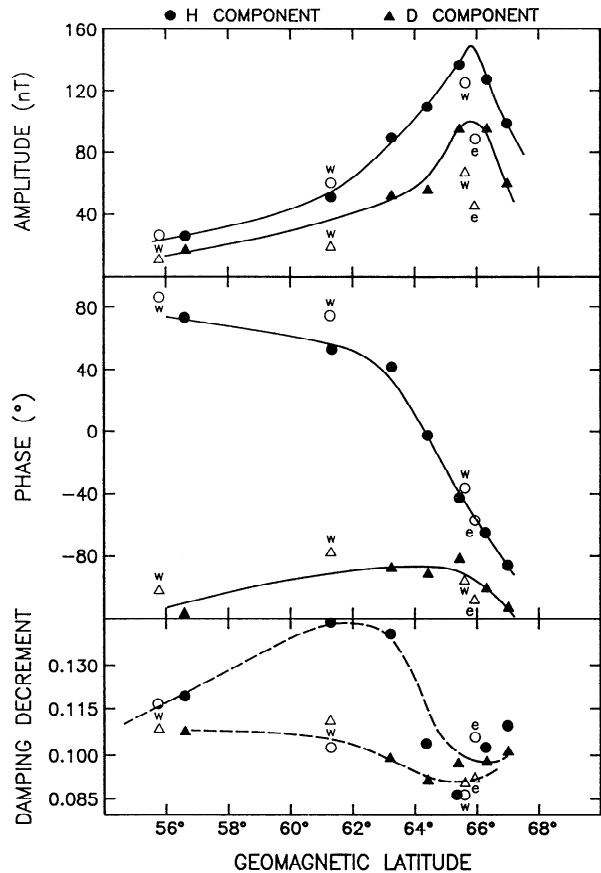


Figure 8. Latitude profiles of the parameters of the post-1419 UT pulsation in the Scandinavian sector; w and e indicate stations west and east respectively, of the meridian line. Solid symbols represent H component (circles) and D component (triangles); open symbols represent the same for w and e stations.

MARIA (EDFL DATA) Equivalent overhead currents
 Propagation 0.2 deg/sec west, step 10 s
 14-Mar-1990 14:11:00-14:18:00

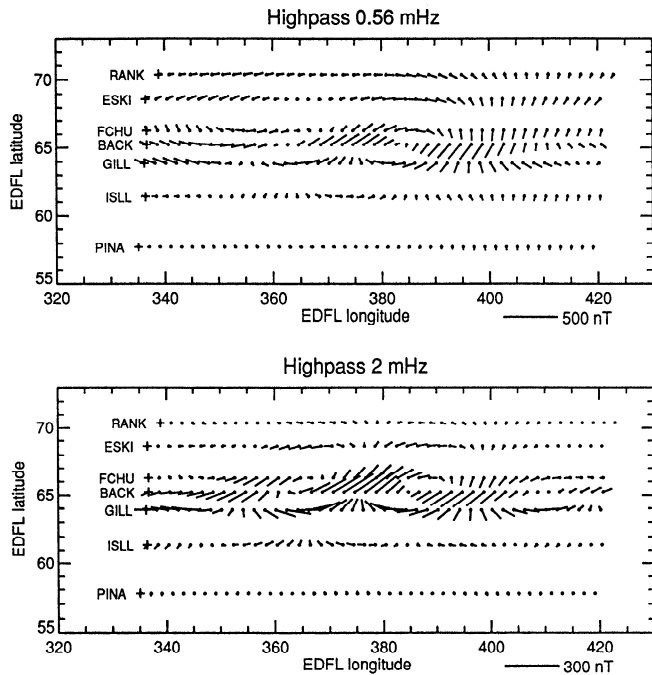


Figure 9. MARIA latitudinal line horizontal equivalent disturbance current vectors plotted as a function of time. Data were high-pass filtered with cutoff frequencies of (top) 0.56 MHz and (bottom) 2 MHz.

The compressional disturbance during 1411 to 1417 was more broadband than was the toroidal response. The latter oscillation was at a slightly higher frequency prior to 1417 than thereafter. The frequency and damping decrement found for the decaying phase were 4.45 mHz (225 s) and 0.08, respectively. Following the procedure described above in the analysis of the Scandinavian sector data, estimates of Σ_p at the footprint of the GOES 7 field line were obtained. Among the contributions to the uncertainty of this estimation is the distortion of the geomagnetic field line from dipolar in this local time sector. In light of this uncertainty the result for Σ_p can be stated as greater than 4 S for a fundamental along the field line and less than 3 S for the second harmonic. Given that the *Wallis and Budzinski* [1981] model predicts a value approaching 10 S, these results suggest a fundamental standing wave along the magnetic field line. This in turn implies a large amplitude disturbance given the location of GOES 7 at 9°N geomagnetic. Using the results of *Cummings et al.* [1969], an H_z component amplitude of 7 nT seen at GOES 7 translates for their m equal to 3 into about 280 nT and 80 nT just above the *E* region for fundamental and second harmonic oscillations on the field line, respectively. Given the position of GOES 7 and the amplitude of the ISLL and GILL *X* component responses, it seems more likely that the oscillation was in the second harmonic than in the fundamental, even though this leaves us with a problem in understanding the Σ_p results.

Energetic Particle Data

There remains one further piece of evidence. The Los Alamos particle instruments on the geosynchronous space-

14-Mar-1990 MEM spectra

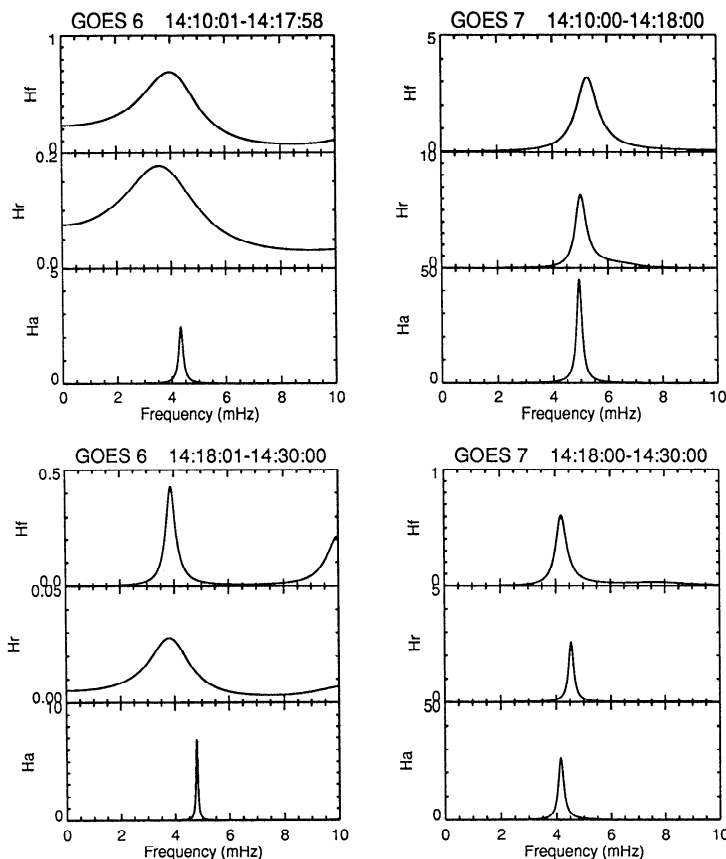


Figure 10. MEM spectra of the (left) GOES 6 and (right) GOES 7 magnetometer data.

craft 1987-097, 1984-129, and 1989-046 recorded oscillations in the energetic electron counts. The modulation of the counts increased with electron energy to beyond 500 keV. Variations in energetic proton counts were much less pronounced. Satellite 1987-097 was in the postnoon sector close to the field lines of the Scandinavian meridian line. Here the count oscillation had a period just under 300 s, not very different from the 326-s period observed in Scandinavia. Analysis of the 1987-097 data (G.D. Reeves, personal communication, 1992) indicates an "injection" at 1406+ in the immediate postnoon sector. These data seem to have some relationship to our event, although we have not yet devised a linking mechanism.

Discussion and Conclusions

We now summarize our findings so as to clearly outline the train of events. BARS and SABRE, which were in the dawn and postnoon sectors, respectively, simultaneously obtained backscatter suggestive of either ringing field lines or of a field line resonance driven by a cavity or waveguide mode. Pulsation activity was also recorded in the ground-based magnetometer arrays which were near the viewing areas of these radars. The event was, however, more complicated than suggested by the BARS and SABRE RTI plots and is not well represented by the global waveguide-mode-excited field line resonance model as currently developed.

The Scandinavian magnetometer records show a pulsation beginning at about 1405. The pulsation amplitude varied in a complex way until about 1419, after which the magnetic disturbance records decayed as simple damped oscillations. Curve fitting showed the pulsation period in this sector to be 326 s (3.07 mHz) at all latitudes. Magnetic records from the United Kingdom sector, however, indicated a change of pulsation structure between Scandinavia and the United Kingdom, i.e., a change with longitude, at least at the lower latitudes.

The variation of the pulsation phase and amplitude with latitude in Scandinavia during the decay phase and the decay rates observed are consistent with a decaying field line resonance into which no energy was being coupled to compensate for ionospheric damping. Estimates of the height-integrated Pedersen conductivity Σ_p indicated the resonance was in the fundamental mode along the field line and that Σ_p was about 5 S. This compares with approximately 8 S from the *Wallis and Budzinski* [1981] model. The SABRE data indicated an eastward phase propagation of the pulsation corresponding to m equal to 5 to 8, although the magnetometer data suggested a value closer to 3. The latter value, however, has a large uncertainty.

The MARIA meridian magnetometer chain running through Churchill was in the dawn sector. These instruments observed a pulsationlike activity beginning at about 1407. During the interval 1412 to 1417 a traveling vortex structure passed over the line. Thereafter, there was an interval during which the disturbance decayed in a complex and, as yet, undecomposed way. A component at approximately 4.5 mHz appears in a number of spectra for the lower-latitude magnetograms (ISLL, GILL, and BACK). Curve fitting yielded a frequency of 4.4 mHz. DMSP data indicate that the traveling vortex structure was deep within the magnetosphere well away from the magnetopause.

GOES 7 was 9° above the magnetic equatorial plane on a field line which, according to the *Tsyganenko* [1989] model, was between those of ISLL and GILL in radial distance and slightly antisunward of them. The magnetic disturbance was first seen here starting at about 1410. A significant compressional mode disturbance occurred between 1410 and about 1417. This may have been associated with the traveling vortex structure seen more poleward by the Churchill MARIA line. During this interval the amplitude of the azimuthal or toroidal mode increased as toward a plateau. Thereafter, the amplitude decreased as a simple damped wave. In this latter interval the frequency was 4.45 mHz (225 s). The damping rate was consistent with a fundamental oscillation along the magnetic field and a Σ_p of greater than 4 S compared with the *Wallis and Budzinski* [1981] model value of approximately 10 S. The peak amplitude of the toroidal oscillation was about 15 nT peak to peak. If this mode was truly fundamental along the field line, then the disturbance would have to have been large, given the proximity of GOES 7 to the expected position of the magnetic node. From the magnetic amplitude observed on the ground relative to that at the satellite it seems more likely that the wave was a second harmonic, implying Σ_p was less, and perhaps significantly less, than 3 S. If so, then a loss mechanism additional to ionospheric Joule heating would be required.

The period of the GOES 7 oscillation in the dawn sector was 225 s, compared with the postnoon field line resonance period of 326 s. The L shells of these two oscillations were almost of equal value. With filling of the flux tubes with cold plasma between the dawn and postnoon sectors [e.g., *Poulter et al.*, 1984] we would expect the period in Scandinavia to be larger than that of the GOES 7 flux tube for the same harmonic along the field line. Thus the observed period increase implies that the Scandinavian resonance was in the same harmonic along the field line as the oscillation seen by GOES 7. The second harmonic is thus suggested for both.

Consider now the size of the damping decrements determined from the Scandinavian magnetometer data. If a diminishing flow of energy from a compressional waveguide (cavity) mode to the field line resonance occurred, then the measured damping rate would be less than that in the absence of such energy flow, and hence the Σ_p deduced from the damping rate would be larger than the actual value. In order to get an estimate of the resulting error in determining Σ_p , the model time sequences used by *McDiarmid and Allan* [1990] were analyzed, using the method employed above (namely, fitting a single damped sinusoid), over a 20-min interval beginning at 25 min in the timing of *McDiarmid and Allan*, which is after the peak amplitude of the response. This approach follows that adopted above, where the data for the interval prior to 1418 were not used for fitting purposes. In both cases the fitting was confined to the decaying phase of the pulsation. The single-sinusoid fits to their model wave trains yielded a latitudinal response width slightly greater than shown by *McDiarmid and Allan* [1990, Figure 6a] and a damping decrement which varied by a value of about 0.03, whereas the natural damping decrement in the model was 0.075. The former value is that predicted by the model for the driven part of the resonance response in which shear mode energy loss is partly compensated by energy inflow from the waveguide (cavity) mode, whereas the latter value corresponds to the actual damping rate of the shear

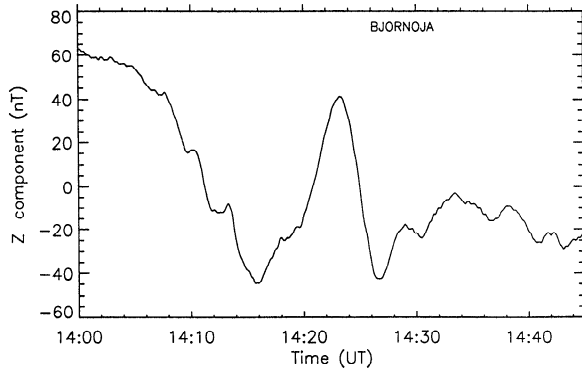


Figure 11. The Bjornoja Z component magnetogram.

mode by the ionosphere. If a similar behavior occurred in the present case, then the implied Σ_p is about 2 S for the fundamental and less for the second harmonic. These values seem much too low. The data therefore suggest significant energy loss via some mechanism additional to ionospheric Joule heating. There is also the possibility that the energy source feeding the shear mode resonance suffered a rapid decay. If a waveguide (cavity) mode was involved, it may have experienced rapid loss of energy down the magnetotail.

Since a damped oscillation (GOES 7) was seen near the equatorward limit of the traveling vortex structure in the dawn sector, one might wonder if a similar vortex structure occurred poleward of Scandinavia in the postnoon sector. Magnetometers exist on both Svalbard and Bjornoja (Bear Island). Svalbard, which is at cleft latitude, was not an

optimum place to look for a vortex system; Bjornoja (geographic 74.5°N, 19.2°E; IGRF 71.1°N, 109.3°E; $L = 9.7$) to the south is better placed. Unfortunately, only the Z component data from this magnetometer exist for this event; they are shown in Figure 11. There is a negative excursion of this component from about 1408 to 1416, when the slope of the disturbance becomes positive, until 1423+. Thereafter, a negative slope exists until 1427- for an event duration of about 20 min. If a sloping line from 60 nT on the left to -30 nT on the right is taken for the background trend, then the event duration is about 24 min.

At first glance one might wonder if this disturbance (1408 to about 1430) bears some resemblance to the Z component plots of *Friis-Christensen et al.* [1988a, Figure 3], only in reverse. In fact, it does not. Not only does the shape differ, but also the duration is too long. Twin vortex structures have a duration of about 10 min [*Friis-Christensen et al.*, 1988a, b; *Glassmeier and Heppner*, 1992], which is significantly shorter than the disturbance in Figure 11. On the other hand, however, if we assume that the disturbance prior to about 1418 had a source different from that thereafter, we see that the Bjornoja Z component during the 1418-1430 interval looks similar to some of the curves of *Friis-Christensen et al.* [1988a, Figure 3]. The evidence is not sufficient to draw a conclusion, but one is left with the suggestion that a traveling vortex structure may have passed over this sector during this interval. Other similar events need to be found and analyzed to resolve this question.

J. C. Samson (personal communication, 1993) has suggested that the dawn sector traveling vortex structure may

GLOBAL SYNOPSIS OF THE PULSATION EVENT

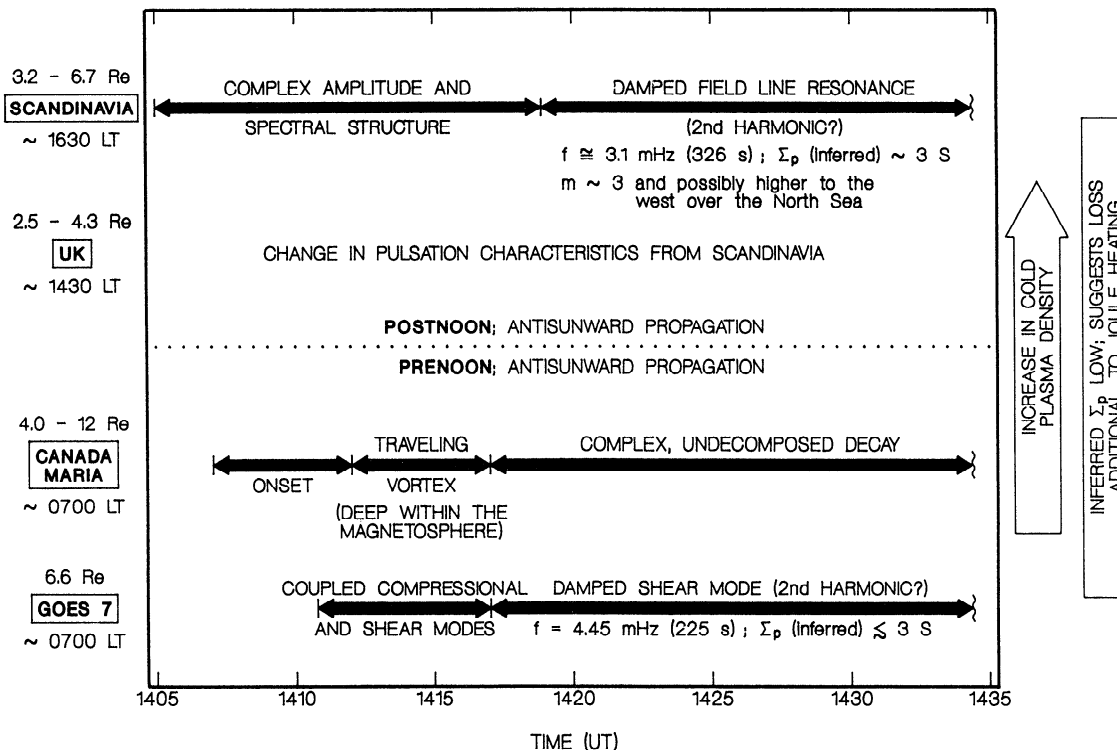


Figure 12. A pictorial representation of the salient features of the March 14, 1990, pulsation event.

have been the result of the nonlinear development of a Kelvin-Helmholtz instability generated by the velocity shear in a large-amplitude field line resonance structure, as proposed by Rankin *et al.* [1993]. Evaluation of this possibility requires further detailed analysis and modeling of this and perhaps other events. However, we note that there is no evidence in Figure 4 of a field line resonance prior to and contiguous with the vortex signature.

Figure 12 is a pictorial representation of the salient features discussed above. The relative timing of the various aspects of the event are clearly seen. In Figure 12, bottom (morning sector), the MARIA and GOES 7 observations in the same time sector are represented. In Figure 12, top (afternoon sector), we see the timing of the damped field line resonance and its precursor. The local time sector of each of the observations is shown on the left-hand side, and some implications of the analysis are recorded on the right-hand side. The asymmetry of the magnetosphere's response relative to the noon meridian is clear to see. This asymmetry does not correspond to what we expect from the model of field line resonances excited by a waveguide mode. However, it is also known that Pc 5 occurrence and polarization characteristics are asymmetric about noon [Rostoker and Sullivan, 1987]. Thus while Figure 11 illustrates the global relationship of the various aspects of our event, the understanding of that relationship remains to be determined.

Thus it is that we have seen an apparent traveling vortex structure in the dawn sector simultaneously with the observation of a complex pulsation in the postnoon sector. What is the cause or causes of this asymmetry about the noon meridian? Other questions also arise. The vortex system was deeply embedded in the magnetosphere. Why was this so? Evidence of longitudinal gradients in these responses was found. What are the causes of these gradients? If the traveling vortex structure was a driven response, then we would expect a transient in its wake. If what was seen was this transient, then its structure was not clearly discernible. Why? On the other hand, GOES 7 at the equatorward side of the traveling vortex observed the excitation of a toroidal oscillation followed by a clear signature of simply damped oscillation. The latter occurred at the same time as the confusing wake behavior seen at higher latitudes. What is the relationship between these two responses? Finally, what is the relationship of the Los Alamos high-energy electron data to this event? Further work is obviously required to address these questions.

Acknowledgments. We would like to thank David Milling for supplying the SAMNET data, Hermann Luhr for supplying the EISCAT magnetometer cross data, and G. D. Reeves for providing the Los Alamos geosynchronous satellite particle data. We appreciate being able to access the JHU/APL on-line neural network data. The SABRE Wick radar is operated by the Ionospheric Physics group of the University of Leicester. SAMNET is deployed and operated by the University of York. The EISCAT magnetometer cross is a joint enterprise of the Finnish Meteorological Institute, the Sodankyla Geophysical Observatory, and the Technical University of Braunschweig. The CANOPUS instrument array was constructed by the Canadian Space Agency (CSA) to the specifications of the Canadian space science community and is maintained and operated by the CSA for that community. W.A. was supported by contract CO1226 of the New Zealand Foundation for Research, Science and Technology.

The Editor thanks E. Nielsen and R. A. Greenwald for their assistance in evaluating this paper.

References

- Allan, W., E. M. Poulter, K.-H. Glassmeier, and H. Junginger, Spatial and temporal structure of a high-latitude transient ULF pulsation, *Planet. Space Sci.*, **33**, 159, 1985.
- Allan, W., E. M. Poulter, and S. P. White, Hydromagnetic wave coupling in the magnetosphere - plasmopause effects on impulse-excited resonances, *Planet. Space Sci.*, **34**, 1189, 1986a.
- Allan, W., S. P. White, and E. M. Poulter, Impulse-excited hydromagnetic cavity and field line resonances in the magnetosphere, *Planet. Space Sci.*, **34**, 371, 1986b.
- Allan, W., E. M. Poulter, and S. P. White, Hydromagnetic wave coupling in the magnetosphere - magnetic fields and Poynting fluxes, *Planet. Space Sci.*, **35**, 1181, 1987.
- Baumjohann, W., H. Junginger, G. Haerendel, and O. H. Bauer, Resonant Alfvén waves excited by a sudden impulse, *J. Geophys. Res.*, **89**, 2765, 1984.
- Crowley, G., W. H. Hughes, and T. B. Jones, Observational evidence of cavity modes in the Earth's magnetosphere, *J. Geophys. Res.*, **92**, 12,233, 1987.
- Crowley, G., W. H. Hughes, and T. B. Jones, Correction to "Observational evidence of cavity modes in the Earth's magnetosphere" by Crowley, G., W. H. Hughes and T. B. Jones, *J. Geophys. Res.*, **94**, 1555, 1989.
- Cummings, W. D., R. J. O'Sullivan, and P. J. Coleman, Jr., Standing Alfvén waves in the magnetosphere, *J. Geophys. Res.*, **74**, 778, 1969.
- Friis-Christensen, E., M. A. McHenry, C. R. Clauer, and S. Vennerstrom, Ionospheric traveling convection vortices observed near the polar cleft: A triggered response to sudden changes in the solar wind, *Geophys. Res. Lett.*, **15**, 253, 1988a.
- Friis-Christensen, E., S. Vennerstrom, C. R. Clauer and M. A. McHenry, Irregular magnetic pulsations in the polar cleft caused by traveling ionospheric convection vortices, *Adv. Space Res.*, **8**(9), 311, 1988b.
- Glassmeier, K.-H., and C. Heppner, Traveling magnetospheric convection twin vortices: Another case study, global characteristics, and a model, *J. Geophys. Res.*, **97**, 3977, 1992.
- Grant, I. F., D. R. McDiarmid, and A. G. McNamara, A class of high-*m* pulsations and its auroral radar signature, *J. Geophys. Res.*, **97**, 8439, 1992.
- Greenwald, R. A., W. Weiss, E. Nielsen, and N. R. Thomson, STARE, a new radar auroral backscatter experiment in northern Scandinavia, *Radio Sci.*, **13**, 1021, 1978.
- Hughes, W. J., and D. J. Southwood, An illustration of modification of geomagnetic pulsation structure by the ionosphere, *J. Geophys. Res.*, **81**, 3241, 1976.
- Inhester, B., Numerical modeling of hydromagnetic wave structure in the magnetosphere, *J. Geophys. Res.*, **92**, 4751, 1987.
- Kivelson, M. G., and D. J. Southwood, Coupling of global magnetospheric MHD eigenmodes to field line resonances, *J. Geophys. Res.*, **91**, 4345, 1986.
- Krauss-Varban, D., and V. L. Patel, Numerical analysis of the coupled hydromagnetic wave equations in the magnetosphere, *J. Geophys. Res.*, **93**, 9721, 1988.
- Lee, D.-H., and R. L. Lysak, Impulsive excitation of ULF waves in the three-dimensional dipole model: The initial results, *J. Geophys. Res.*, **96**, 3479, 1991.
- Luhr, H., S. Thurey, and N. Klockner, The EISCAT magnetometer cross: Operational aspects - first results, *Geophys. Surv.*, **6**, 305, 1984.

- Lysak, R. L., and D.-H. Lee, Response of the dipole magnetosphere to pressure pulses, *Geophys. Res. Lett.*, **19**, 937, 1992.
- McDiarmid, D. R., and W. Allan, Simulation and analysis of auroral radar signatures generated by a magnetospheric cavity mode, *J. Geophys. Res.*, **95**, 20,911, 1990.
- McNamara, A. G., D. R. McDiarmid, G. J. Sofko, J. A. Koehler, P. A. Forsyth, and D. R. Moorcroft, BARS - A dual bistatic auroral radar system for the study of electric fields in the Canadian sector of the auroral zone, *Adv. Space Res.*, **2**(7), 145, 1983.
- Newell, P. T., S. Wing, C.-I. Meng, and V. Sigillito, The auroral oval position, structure, and intensity of precipitation from 1984 onward: An automated on-line data base, *J. Geophys. Res.*, **96**, 5877, 1991.
- Newton, R. S., D. J. Southwood, and W. J. Hughes, Damping of geomagnetic pulsations by the ionosphere, *Planet. Space Sci.*, **26**, 201, 1978.
- Nielsen, E., Observations of sunward propagating waves on the magnetopause, *J. Geophys. Res.*, **89**, 9095, 1984.
- Nielsen, E., W. Guttler, E. C. Thomas, C. P. Stewart, T. B. Jones, and A. Hedburg, SABRE-A new radar auroral backscatter experiment, *Nature*, **304**, 712, 1983.
- Nopper, R. W., W. J. Hughes, C. G. MacLennan, and R. L. McPherron, Impulse-excited pulsations during the July 29, 1977, event, *J. Geophys. Res.*, **87**, 5911, 1982.
- Potemra, T. A., H. Luhr, L. J. Zanetti, K. Takahashi, R. E. Erlandson, G. T. Marklund, L. P. Block, L. G. Blomberg, and R. P. Lepping, Multisatellite and ground-based observations of transient ULF waves, *J. Geophys. Res.*, **94**, 2543, 1989.
- Poulter, E. M., Pc 5 micropulsation resonance regions observed with the STARE radar, *J. Geophys. Res.*, **87**, 8167, 1982.
- Poulter, E. M., and W. Allan, Transient ULF pulsation decay rates observed by ground based magnetometers: The contribution of spatial integration, *Planet. Space Sci.*, **33**, 607, 1985.
- Poulter, E. M., W. Allan, J. G. Keys, and E. Nielsen, Plasma-trough ion mass densities determined from ULF pulsation eigenperiods, *Planet. Space Sci.*, **32**, 1069, 1984.
- Rankin, R., B. J. Harrold, J. C. Samson, and P. Frycz, The nonlinear evolution of field line resonances in the Earth's magnetosphere, *J. Geophys. Res.*, **98**, 5839, 1993.
- Rostoker, G., and B. T. Sullivan, Polarization characteristics of Pc 5 magnetic pulsations in the dusk hemisphere, *Planet. Space Sci.*, **35**, 429, 1987.
- Rufenach, C. L., R. L. McPherron, and J. Schaper, The quiet geomagnetic field at geosynchronous orbit and its dependence on solar wind dynamic pressure, *J. Geophys. Res.*, **97**, 25, 1992.
- Samson, J. C., J. A. Jacobs, and G. Rostoker, Latitude-dependent characteristics of long-period geomagnetic pulsations, *J. Geophys. Res.*, **76**, 3675, 1971.
- Samson, J. C., B. J. Harrold, J. M. Ruohoniemi, R. A. Greenwald, and A. D. M. Walker, Field line resonances associated with MHD waveguides in the magnetosphere, *Geophys. Res. Lett.*, **19**, 441, 1992.
- Tsyganenko, N. A., A magnetospheric magnetic field model with a warped tail sheet, *Planet. Space Sci.*, **37**, 5, 1989.
- Walker, A. D. M., Modelling Pc 5 structure in the magnetosphere, I, Toroidal motion and associated fields, *Res. Rep. R1/79*, Dep. of Phys., Univ. of Natal, Durban, S.Afr., 1979.
- Walker, A. D. M., Modelling of Pc 5 pulsation structure in the magnetosphere, *Planet. Space Sci.*, **28**, 213, 1980.
- Walker, A. D. M., M. J. Ruohoniemi, K. B. Baker, R. A. Greenwald, and J. C. Samson, Spatial and temporal behavior of ULF pulsations observed by the Goose Bay HF radar, *J. Geophys. Res.*, **97**, 12,187, 1992.
- Wallis, D. D., and E. E. Budzinski, Empirical models of height-integrated conductivities, *J. Geophys. Res.*, **86**, 125, 1981.
- Wallis, D. D., J. R. Burrows, T. J. Hughes, and M. D. Wilson, Eccentric dipole coordinates for MAGSAT data presentation and analysis of external current effects, *Geophys. Res. Lett.*, **9**, 353, 1982.
- Yeoman, T. K., D. K. Milling, and D. Orr, Pi2 pulsation polarization patterns on the U.K. Sub-auroral Magnetometer Network (SAMNET), *Planet. Space Sci.*, **38**, 589, 1990.
- Yumoto, K., K. Takahashi, T. Sakurai, P. R. Sutcliffe, S. Kokubun, H. Luhr, T. Saito, M. Kuwashima, and N. Sato, Multiple ground-based and satellite observations of global Pi 2 magnetic pulsations, *J. Geophys. Res.*, **95**, 15,175, 1990.
- Zhu, X. M., and M. G. Kivelson, Analytic formulation and quantitative solutions of the coupled ULF wave problem, *J. Geophys. Res.*, **93**, 8602, 1988.

W. Allan, National Institute of Water and Atmospheric Research, P.O. Box 31-311, Lower Hutt, New Zealand. (e-mail: Internet.srgpwx@grace.dsr.govt.nz)

I. F. Grant, Department of Physics, University of Western Ontario, London, Ontario, Canada N6A 3K7. (e-mail: SPAN.canlon::grant)

D. R. McDiarmid, Herzberg Institute of Astrophysics, National Research Council, Ottawa, Ontario, Canada K1A 0R6. (e-mail: Internet.mcdiarmid@dan.sp-agency.ca, SPAN.canott::mcdiarmid)

T. K. Yeoman, Ionospheric Physics Group, Department of Physics and Astronomy, Leicester University, Leicester, LE1 7RH, England. (e-mail: Internet.yxo@ion.le.ac.uk)

(Received June 3, 1993; revised November 16, 1993; accepted January 12, 1994.)